

High-energy (56 MeV) oxygen implantation in Si, GaAs, and InP

S. J. Pearton, B. Jalali, and J. M. Poate
AT&T Bell Laboratories, Murray Hill, New Jersey 07974

J. D. Fox and K. W. Kemper
Department of Physics, Florida State University, Tallahassee, Florida 32306

C. W. Magee
Evans East, Inc., Plainsboro, New Jersey 08536

K. S. Jones
University of Florida, Gainesville, Florida 32611

(Received 25 June 1990; accepted for publication 23 August 1990)

The depth profiles measured by secondary-ion mass spectrometry of 56 MeV oxygen ions implanted into Si, GaAs, and InP are reported. Most of the oxygen is contained within a sharp (full width at half maximum $\sim 2 \mu\text{m}$) non-Gaussian profile centered at $\sim 31 \mu\text{m}$ in GaAs, $\sim 36 \mu\text{m}$ in InP, and $\sim 46 \mu\text{m}$ in Si, with the distribution skewed towards greater depths. The experimental projected ranges appear to be 10% larger than theoretical predictions. Changes in the electrical, optical, and structural properties of the material were measured by transmission electron microscopy (TEM), photoluminescence, and spreading resistance profiling. In the as-implanted Si, the maximum perturbation in the electrical properties occurs at $\sim 37 \mu\text{m}$. No defects are visible by TEM in any of the as-implanted semiconductors for oxygen ion doses of $1.35 \times 10^{15} \text{ cm}^{-2}$ but the photoluminescent intensity in GaAs and InP is reduced by more than an order of magnitude as a result of this type of implantation.

There is increasing interest in the use of MeV ion implantation for both current and future device fabrication technologies. For example, in III-V devices, MeV implantation can be used to form buried isolation layers or buried channel charge-coupled devices (CCDs),¹⁻³ while in Si similar implants are used for complementary metal-oxide semiconductor (CMOS) well formation, the formation of buried collectors in bipolar transistors, buried interconnects, or for deep gettering layers.⁴⁻⁹ In addition, there have been several recent reports of the use of 120 MeV oxygen ion irradiation for reducing the critical currents and transition temperatures of various oxide superconductors.^{10,11} To apply high-energy implantation in any of these practical applications it is necessary to have accurate range parameters for the ions.^{12,13} There is simply a lack of experimental data for the range statistics of very high-energy (≥ 20 MeV) implants in semiconductors. The most complete work to date on implants at these energies comes from La Ferla *et al.*^{14,15} who measured the activation and diffusion characteristics of 15–50 MeV boron ions implanted into Si.

In this letter we report on the depth distributions of 56 MeV oxygen ions implanted into Si, GaAs, and InP, together with a measurement of the effect of these implants on the electrical properties of Si. Finally, the effect of these high-energy ions on the optical properties of the GaAs and InP are measured by photoluminescence spectroscopy.

The substrates used were all cut from 2-in.-diam boules. The Si was *n*-type, (100) Czochralski-grown material with resistivity $5 \Omega \text{ cm}$. The GaAs was nominally undoped (100) material with resistivity $2 \times 10^7 \Omega \text{ cm}$, grown by the liquid-encapsulated Czochralski (LEC) technique. Finally, the (100) InP was Fe-doped, semi-

insulating ($> 10^7 \Omega \text{ cm}$) material also grown by the LEC method. We chose oxygen as the implant species because it is widely used as the bombarding ion for creating high-resistivity regions in both GaAs and InP for device isolation purposes, and at very high doses oxygen implantation is used to form buried SiO_2 layers in Si.

The samples were bombarded with 6^+ oxygen ions for approximately 30 min so that a total of 1.35×10^{15} ions entered the surface in each case. The terminal voltage was 8.0 MV and the injected ion beam was oxygen in the -1 charge state. The beam is $+6$ after stripping in the terminal, so that the final energy was 56 MeV. The samples were mounted on the massive target rod of a scattering chamber, with the sample normal parallel to the beam direction to within 5° . Although the average power dissipated by the beam over the target area (roughly 1 cm^2) was close to 5 W, the target temperature was only slightly warm to the touch after bombardment. The error on the energy was $\pm 100 \text{ keV}$ and in the dose was $\pm 1\%$.

The depth profiles of the implanted ions were measured by secondary-ion mass spectrometry (SIMS) in a Perkin Elmer 6300 system using 8 keV Cs^+ ion bombardment. This beam was rastered over areas of $300 \times 300 \mu\text{m}^2$ or $600 \times 600 \mu\text{m}^2$, with negatively charged secondary ions detected only from the central $90 \times 90 \mu\text{m}^2$ or $180 \times 180 \mu\text{m}^2$ regions, respectively. The beam current used was $1 \mu\text{A}$ at an impact angle of 60° , and no charge neutralization was employed. The depth axes were established after the analyses by measuring the sputtered crater depths with a calibrated profilometer. This required very careful setup of the profilometer to ensure it was within its linear operating range. These are unusually deep profiles for SIMS measurement, and required up to 6 h of sputter time. The two

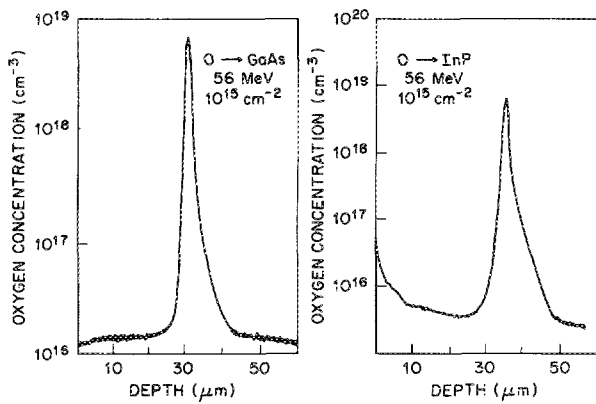


FIG. 1. Atomic profiles of 56 MeV oxygen ions implanted into GaAs (at left) or InP (at right) to a dose of 10^{15} cm^{-2} .

different raster sizes mentioned above were used in order to ensure the accuracy and consistency of the SIMS analysis. Changes in the free-carrier profile in the Si sample as a result of the oxygen implantation were obtained from spreading resistance measurements using an angle-lapped geometry. Photoluminescence (PL) measurements were performed at 300 K using an Ar^+ ion laser as an excitation source. We also looked for the presence of buried damage layers in all three materials using cross-sectional transmission electron microscopy (TEM). In these cases the samples were prepared by a combination of mechanical and chemical thinning.

Figure 1 shows the atomic profiles of 56 MeV oxygen ions implanted into both GaAs (at left) and InP (at right) at a dose of $\sim 1.35 \times 10^{15} \text{ cm}^{-2}$. The shape of both implant distributions is markedly non-Gaussian, with a delta function rise in concentration at depths around 30–35 μm . The skewness towards greater depths is quite reproducible and does not appear to be an artifact of the SIMS analysis. These tails were evident with both Cs^+ beam raster sizes used and do not appear to be artifacts of the SIMS analysis. At these high energies the ions will follow relatively straight paths with electronic stopping dominant over most of the range. This leads to a sharp peak in the oxygen distribution, with little contribution from the large-angle deflections significant at conventional energies. The sharp peak in the range profile is therefore fairly typical of high energy implants. The straggle in the profile can arise from comparable contributions from both electronic and nuclear energy loss straggling.¹³ The profile shapes with the high depth skew are similar to those reported by La Ferla *et al.*^{14,15} One probable explanation for this skewness is a channeling effect. The background levels of $\sim 10^{16} \text{ cm}^{-3}$ are determined by the sensitivity of the SIMS technique and depend primarily on the oxygen sticking probability arising from the ambient atmosphere. The ratio of the peak concentration of each profile to the concentration at the surface is therefore $\geq 10^3$ in each case. For 50 MeV boron implantation into Si similar values of this ratio were found.^{14,15}

The SIMS profile of the 56 MeV oxygen implantation into Si is shown in Fig. 2 (at left). The same profile fea-

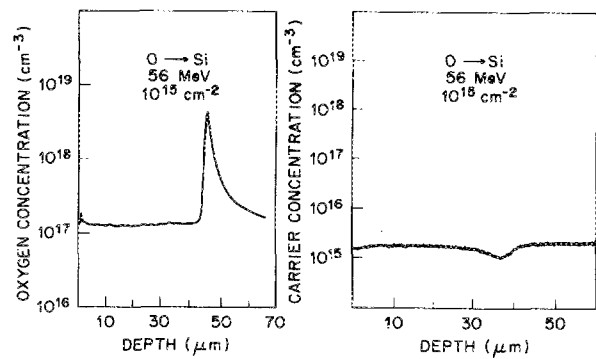


FIG. 2. Atomic profile of 56 MeV oxygen ions implanted into Si to a dose of 10^{15} cm^{-2} (at left) and carrier profile in 5 $\Omega \text{ cm}$, *n*-type Si after the same implant (at right).

tures are seen as for the GaAs and InP. The profile is characterized by a very sharp rise in oxygen concentration followed by a tail deeper into the substrate. The background concentration of oxygen detected by SIMS in Si is much higher than for the III-V materials and is an artifact of the SIMS technique arising from the enhanced oxygen sticking probability. An estimate of the depth of the disorder distribution in the Si can be obtained from a measurement of the free carrier profile after implantation. This is also shown in Fig. 2 (at right). Nuclear stopping by ions in semiconductors creates deep level centers which trap free carriers in the material. The most significant damage occurs in the region where the ions have slowed down to low energies. In our samples the maximum change in the carrier concentration occurs at $\sim 37 \mu\text{m}$. If we correlate this with the damage distribution then the latter peaks at a considerably shallower depth than the ion distribution ($\sim 46 \mu\text{m}$). Although the damage is expected to be shallower than the ion profile, this is a rather large effect. Damage is created by elastic collisions which occur mainly at the end of the ion path. In very high-energy implants electrical damage and the impurity profile would be expected to be closely correlated. At conventional energies, the peak in the damage distribution also occurs at shallower depths than the peak in the range distribution.¹³ It is not clear however that such a comparison is valid at high energies, and this point is currently under investigation.

Linear plots of the oxygen profiles in GaAs, InP, and Si are shown in Fig. 3. These clearly show that essentially all of the implanted oxygen resides in a well-defined region in the distributions. The peak in the oxygen profile occurs at $\sim 31 \mu\text{m}$ for GaAs, $\sim 36 \mu\text{m}$ for InP, and $\sim 46 \mu\text{m}$ for Si. These can be compared to the projected ranges for 56 MeV oxygen ions in these materials predicted by the projected range theory algorithm PRAL.¹⁶ This is equivalent to solving a Boltzmann transport equation for the ions. For GaAs the projected range of the oxygen is predicted to be 29 μm , with a longitudinal straggle of 1.1 μm . Similarly, for InP the projected range is estimated to be 32.2 μm while for Si the range is 43.2 μm . In each case our experimental values are larger by $\leq 10\%$ than the predicted ranges.

The effect of the oxygen implantation on the optical

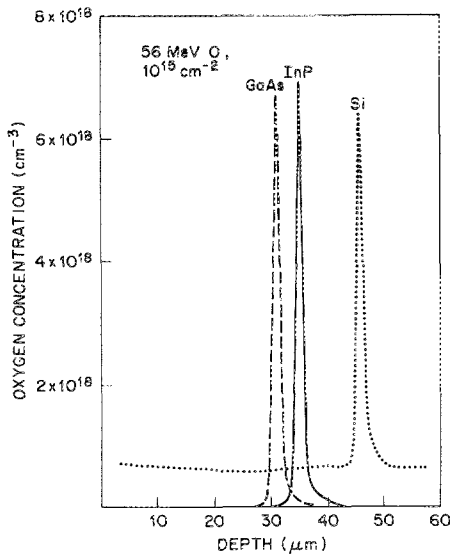


FIG. 3. Linear plots of atomic profiles of 56 MeV oxygen ions implanted into GaAs, InP, and Si to a dose of 10^{15} cm^{-2} .

properties of GaAs and InP was examined using photoluminescence measurements. Figure 4 shows PL spectra before and after oxygen implantation to a dose of 10^{15} cm^{-2} . The diffusion length of minority carriers in both materials is $\leq 1 \mu\text{m}$, but there is enough lattice damage introduced into this region to reduce the PL intensity by more than an order of magnitude. This indicates that even at the highest

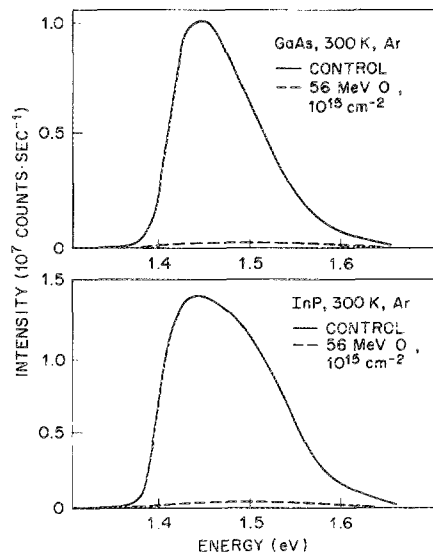


FIG. 4. Photoluminescence spectra from GaAs (at top) and InP (at bottom) before and after implantation with 56 MeV oxygen ions to a dose of 10^{15} cm^{-2} .

ion energies there is enough nuclear stopping occurring to significantly alter the luminescent intensity of both GaAs and InP. Companion samples were examined by cross-sectional TEM but no defects were visible either near the surface or at the end of the ion ranges. Similar results were obtained with the implanted Si sample. We did not examine the samples after a subsequent high-temperature anneal, where agglomeration of point defects might have created a buried damage layer. The fact that we did not observe any defects by TEM for a dose of 10^{15} cm^{-2} appears to be consistent with the data of El-Ghor *et al.* for lower energy (1.25 MeV) Si^+ implantation into Si.¹⁷

In summary, we have measured the atomic profiles for very high-energy (56 MeV) oxygen implants into GaAs, InP, and Si. The profiles have similar shapes, with most of the oxygen contained within a skewed, non-Gaussian profile centered at $\sim 31 \mu\text{m}$ in GaAs, $\sim 36 \mu\text{m}$ in InP, and $\sim 46 \mu\text{m}$ in Si. The maximum change in the electrical properties of Si occurs at $\sim 37 \mu\text{m}$. For each material the experimental values for the projected range are $\sim 10\%$ higher than theoretical predictions. No defects were observed by TEM in the as-implanted samples, but enough lattice disorder is introduced into the near-surface ($\leq 1 \mu\text{m}$) region of both GaAs and InP to significantly degrade their optical properties.

Two of the authors (J. D. F. and K. W. K.) are supported by the State of Florida and the National Science Foundation.

- ¹H. B. Dietrich, Proc. SPIE Conf. 530, 30 (1985).
- ²P. E. Thompson, Proc. Electrochemical Society meeting on Ion Implantation and Dielectrics for Elemental and Compound Semiconductors, Hollywood, FL, Oct. 1989 (in press).
- ³R. G. Wilson, J. Appl. Phys. 60, 2797 (1987).
- ⁴N. Cheung, Proc. SPIE Conf. 530, 2 (1985).
- ⁵D. C. Ingram, J. A. Baker, D. A. Walsh, and E. M. Strathman, Nucl. Instrum. Methods B 21, 460 (1987).
- ⁶D. Pramanik and A. N. Saxena, Nucl. Instrum. Methods B 10/11, 493 (1985).
- ⁷G. A. Sai-Halasz, M. R. Wordeman, and E. H. Dennard, IEEE Electron. Devices ED-29, 725 (1982).
- ⁸M. I. Current, R. A. Martin, K. Doganis, and R. H. Bruce, Proc. SPIE Conf. 530, 117 (1985).
- ⁹P. F. Byrne, N. W. Cheung, and D. K. Sadana, Appl. Phys. Lett. 41, 537 (1982).
- ¹⁰A. Iwase, M. Masaki, T. Iwata, S. Sasaki, and T. Nihira, Jpn. J. Appl. Phys. 27, L2071 (1988).
- ¹¹A. Iwase, M. Watanabe, T. Iwata, and T. Nihira, Jpn. J. Appl. Phys. 28, L1939 (1989).
- ¹²J. F. Ziegler, Nucl. Instrum. Methods B 6, 270 (1985).
- ¹³J. P. Biersack, Nucl. Instrum. Methods B 35, 205 (1988).
- ¹⁴A. La Ferla, E. Rimini, G. Ciavola, and G. Ferla, Nucl. Instrum. Methods Phys. Res. B 37/38, 951 (1989).
- ¹⁵A. La Ferla, A. DiFranco, E. Rimini, G. Ciavola, and G. Ferla, Mat. Sci. Eng. B 2, 69 (1989).
- ¹⁶J. P. Biersack, Nucl. Instrum. Methods 182/183, 199 (1981).
- ¹⁷M. K. El-Ghor, O. W. Holland, C. W. White, and S. J. Pennycook, J. Mater. Res. 5, 352 (1990).